Improved Stability of Organic-Inorganic Composite Emitting Film with Sol-Gel Encapsulated Eu Complex

Takeshi Fukuda*[,a], Shuhei Yamauchi[a], Zentaro Honda[a], Naoto Kijima[b], Norihiko Kamata[a]

[a] *Department of Functional Materials Science, Saitama University, 255 Shimo-Ohkubo, Sakura-ku, Saitama-shi, Saitama 338-8570, Japan*
[b] *Mitsubishi Chemical Group, Science and Technology Research Center, Inc., 1000 Kamoshida-cho, Aoba-ku, Yokohama, Kanagawa 227-8502, Japan.*

Abstract

A high-stability organic-inorganic composite emitting film has been realized via a sol-gel process using an optimized silane alkoxide and Eu-complex. We found that the long-term and thermal stabilities were improved by using a combined starting solution of phenyltrimethoxysilane and tetrametoxysilane as encapsulating agent. The resulting emitting film exhibited sharp red-luminescence under ultraviolet (UV) excitation and a high transparency in the visible wavelength region. In addition, no decrease in photoluminescence (PL) quantum yield was observed after thermal treatment up to 180 ℃, and the reduction in PL intensity during UV irradiation was suppressed by encapsulating the Eu-complex within the sol-gel derived silica glass.

Key words: Eu-complex, Sol-gel process, Encapsulation, Photoluminescence quantum yield, Thermal stability, Long term stability

1. Introduction

Phosphors have been widely investigated as white light-emitting diodes (LEDs) [1, 2], biosensors [3] and wavelength conversion films for silicon photovoltaic cells [4, 5]. Especially, europium (Eu) complexes have unique spectroscopic characteristics, such as a near-ultraviolet excitation, sharp emission peaks, high photoluminescence (PL) quantum yield, and long luminescence

*Corresponding author. Tel.: +81-48-858-3526; fax: +81-48-858-3526.
Email address: fukuda@fms.saitama-u.ac.jp (Takeshi Fukuda)

lifetimes [6, 7]. Combining with an appropriate ligand to form Eu-complexes improves the absorption coefficient of each Eu ion, and solves the problem of concentration quenching due to the long inter-molecular distance.

One of the most serious problems with Eu-complexes is their long-term stability in the presence of ultraviolet (UV) light irradiation. This is because the strength of the bond between the Eu ion and the organic ligand is lower than that of a conventional inorganic material. Therefore, the chemical structure of the Eu-complex changes under UV-irradiation, resulting in a decrease in the emission intensity [8, 9, 10, 11]. Since in the case of white LEDs, Eu-complexes are necessarily irradiated by an excited UV light source, it is necessary to find a solution to this problem.

Recently, Peng et al. reported a method of encapsulating Eu-complexes as solutions in organic solvent, and demonstrated an improvement in the lifetime by encapsulating by base catalyzed hydrolysis of octyltrimetholysilane [12]. In addition, several researchers have demonstrated that nano-size Eu-complex particles can be realized by encapsulating with sol-gel derived materials [13, 14, 15, 16], and that this leads to an increase in the stability of the photoluminescence (PL) intensity against UV light irradiation [17]. Since sol-gel synthesis, including the final annealing process, can be performed at temperatures below 150 ℃, thermal decomposition of the Eu-complex does not occur during the fabrication process. In addition, a hybrid organic-inorganic emitting film combining organically modified silicate and Eu-complexes has been reported [18].

In this paper, we investigated the influence of the encapsulating agent on the stability of an encapsulated emitting organic-inorganic composite film composed of bis(triphenylphosphine)tris(hexafluoroacetyl acetonato)europium(III) ($Eu(HFA)_3(TPPO)_2$) against UV light irradiation. We used two encapsulating agents, phenyltrimethoxysilane (PTMS) and tetrametoxysilane (TMOS) by adding another silane alkoxide, dimethyldimethoxysilane (DEDMS). We measured the long-term stability while irradiating with UV light with an intensity and a center wavelength of 6.95 mW/cm^2 and 350 nm, respectively. In addition, the relationship between the annealing temperature and the PL quantum yield was also investigated to estimate the improvement in the thermal stability of $Eu(HFA)_3(TPPO)_2$ due to the sol-gel encapsulation technique.

2. Experimental

Figure 1 shows the flowchart of the encapsulation process for $Eu(HFA)_3(TPPO)_2$ via a sol-gel derived silica glass. The synthesis process for $Eu(HFA)_3(TPPO)_2$ was described in a previous paper [19]. At first, $Eu(HFA)_3(TPPO)_2$ powder was added to the encapsulating agents, PTMS:DEDMS for sample A and TMOS:DEDMS for sample B. The resulting solution was then injected into a mixture of distilled water, and ethanol. The concentrations of starting solutions are summarized in Table 1. Prior to injection, the solution was mixed at 25 ℃ for 72 hours (sample A) and 5 hours (sample B) until $Eu(HFA)_3(TPPO)_2$ was completely dissolved. In the case of sample A, the solution was further mixed at 100 ℃ for 3 hours. The hydrolysis rate of silane alkoxide is different for PTMS and TMOS, and therefore an optimal mixing time was selected to achieve a suitable viscosity for the spin-coating process. The rotation speed was maintained at 400 rpm by a magnetic stirrer for all the mixing processes. Finally, the solution was spin-coated at a rotation speed of 2000 rpm for 60 seconds. To investigate the thermal stability of the sol-gel glass encapsulated $Eu(HFA)_3(TPPO)_2$, the fabricated samples were annealed for 2 hours in the temperature range 120 to 220 ℃ using a hotplate. For comparison, $Eu(HFA)_3(TPPO)_2$ powder was dissolved in tetrahydrofuran (THF), and the solution was also spin-coated and annealed under the same conditions as the encapsulated samples. THF is easily removed during annealing above 120 ℃ owing to its low boiling point.

The PL quantum yield was measured by a luminance quantum yield measurement system (QEMS-2000, Systems Engineering Inc.), which consists of an integrated sphere and a UV LED with a center wavelength of 375 nm as an excitation source. The PL quantum yield was determined using a method based upon that originally developed by de Mello et al. [20]. In this approach, the quantum yield was given by the integrated PL intensity of the sample excited by the UV-LED divided by the decrease in the excitation intensity caused by inserting the sample into the integrated sphere. The long-term stability was estimated as the PL intensity change at 613 nm while irradiating with UV light with a center wavelength of 350 nm and an optical intensity of 6.95 mW/cm^2. The optical intensity of the UV light used was the maximum value available in our experimental setup. The PL intensity change and photoluminescence/ photoluminescence excitation (PL/PLE) spectra were measured by a luminance spectrometer (FluoroMax-3, Horiba Jovin Yvon).

3. Results and discussion

Figure 2 shows optical microscopic images of samples A and B. The annealing temperature was fixed at 120 ℃. A mixture of DEDMS was chosen rather than PTMS and TMOS alone, because hydrolysis is more easily achieved with DEDMS [21, 22]. The function of DEDMS is to form a more flexible linear network than the one obtained by hydrolysis of PTMS and TMOS alone. The Eu-complex is incorporated in the sol-gel derived glass matrix at the same time as the hydrolysis and condensation reactions of silane start, and not after the sol-gel glass formation has finished. Therefore, for both samples, we could obtain a transparent and almost crack-free film by using DEDMS during the formation of the silica network around $Eu(HFA)_3(TPPO)_2$. As clearly shown in Fig. 2, a transparent film with a smooth surface was obtained in the case of sample A. The dark regions seen in sample B corresponded to the aggregation of $Eu(HFA)_3(TPPO)_2$. However, such aggregation did not occur in sample A, which was fabricated using PTMS as a silane alkoxide. This is because $Eu(HFA)_3(TPPO)_2$ dissolves directly in PTMS, and therefore does not aggregate during evaporation of the ethanol and distilled water.

The PL and PLE spectra of the sol-gel glass encapsulated $Eu(HFA)_3(TPPO)_2$ and the spin-coated sample are shown in Figs. 3(a) and (b), respectively. The excitation wavelength of the PL spectrum was 350 nm. The PL spectra of samples A and B clearly indicate that the sol-gel glass encapsulated $Eu(HFA)_3(TPPO)_2$ generated sharp red emission with a center wavelength of 613 nm. The peak wavelength of the PL spectrum corresponds to the transition between $^5D_0$ and $^7F_2$ [23, 24].

The excitation spectrum was monitored at 613 nm, corresponding to the peak wavelength of the measured PL spectrum, as shown in Fig. 3(a). All of the samples showed a broad PLE spectrum below 400 nm, suitable for white LEDs with near-violet excitation. However, the PLE spectrum of sample A was shifted toward longer wavelength compared to that of sample B, and the relative PL intensities at 380 nm of samples A and B were 0.89 and 0.70, respectively. In generally, the PLE spectrum of Eu-complexes is affected by the energy transfer from the organic ligand to the Eu^{3+} ion [6]. Therefore, this result indicates that the molecular structure of $Eu(HFA)_3(TPPO)_2$ was changed during the sol-gel process, resulting in the blue-shift of the PLE spectrum.

Figure 4 shows the PL quantum yield of $Eu(HFA)_3(TPPO)_2$ encapsulated

by sol-gel derived silica glasses and the spin-coated sample. All the samples were annealed at temperatures in the range from 120 to 220 ℃ to investigate the thermal stability of the sol-gel glass encapsulated $Eu(HFA)_3(TPPO)_2$. If the organic ligands in $Eu(HFA)_3(TPPO)_2$ are decomposed by the annealing process, the PL quantum yield will decrease due to the low energy-transfer efficiency between the organic ligand and the Eu^{3+} ion. Therefore, we can estimate the thermal stability of $Eu(HFA)_3(TPPO)_2$ by measuring the PL quantum yield. The PL quantum yield of the spin-coated sample was found to rapidly decrease with increasing annealing temperature due to oxidization of the organic ligand structure in the ambient air.

As seen in Fig. 4, both encapsulated samples exhibited enhanced thermal stability during annealing compared to the spin-coated sample. The most important finding is that the PL quantum yield of sample A was almost unaffected by annealing at temperatures less than 180 ℃, and it rapidly decreased above 200 ℃. Since the organic ligand structure of $Eu(HFA)_3(TPPO)_2$ is easily decomposed at 200 ℃, the decrease in the PL quantum yield above 200 ℃ is readily understandable. The fact that no degradation occurred at temperatures less than 180 ℃ indicates that the sol-gel glass protects the $Eu(HFA)_3(TPPO)_2$ against oxygen. Therefore, sol-gel glass encapsulation method using PTMS and DEDMS mixed alkoxide is a useful way to improve the thermal stability. The fact that the PL quantum yield of sample B was lower than that of sample A indicates that the TMOS caused the $Eu(HFA)_3(TPPO)_2$ to decompose during the sol-gel process.

Figure 5 shows the change in the PL intensity for $Eu(HFA)_3(TPPO)_2$ with and without sol-gel glass encapsulation under 350 nm excitation. The optical intensity of the excitation light was fixed at 6.95 mW/cm^2, and the annealing temperature for all samples was 120 ℃. The relative PL intensity of the spin-coated sample decreased under UV irradiation, and became 0.46 after 5400 s. Similar to the annealing temperature dependence of PL quantum yield, the long-term stability against UV light irradiation was also improved by encapsulating using sol-gel derived glass. However, sample B had lower stability than sample A due to structural changes to $Eu(HFA)_3(TPPO)_2$ caused by the presence of TMOS during the sol-gel process. The most important result is that sample A achieved the highest stability in this study, with a relative PL intensity of 0.76 following 5400 s of emission.

As shown in Figs. 4 and 5, sample A has higher stability than sample B, allowing us to conclude that PTMS is a more suitable material for sol-gel glass encapsulation. We subsequently investigated the annealing temperature de-

pendence of the PL intensity change during UV light irradiation of sample A. Figure 6 shows the variation in the PL intensity for annealing temperatures of 120, 140, and 160 ℃. The optical intensity and the center wavelength were 6.95 mW/cm^2 and 350 nm, respectively. In general, higher annealing temperature leads to a higher density of the sol-gel derived glass, and thus a higher encapsulation efficiency. This is thought to be the reason for the smaller decrease in output intensity over time as the annealing temperature is changed from 120 to 140 ℃. However, following annealing at 160 ℃, the PL intensity rapidly decreased, most likely due to changes that occurred to the chemical structure of $Eu(HFA)_3(TPPO)_2$ at this temperature.

In Fig. 7(a), we show UV-visible spectra of sample A for different annealing temperatures. A distinctive absorption peak appears at approximately 350 nm, and is attributed to the organic ligand of $Eu(HFA)_3(TPPO)_2$. Figure 7(b) shows the relationship between the annealing temperature and the absorption coefficient at 350 nm. The absorption coefficient shows no change below 160 ℃, but rapidly decreases for higher temperatures, again indicating a change in the molecular structure of $Eu(HFA)_3(TPPO)_2$.

4. Conclusion

We demonstrated an organic-inorganic composite film composed of $Eu(HFA)_3(TPPO)_2$ encapsulated by sol-gel glasses, and studied its thermal and long-term stability against UV light irradiation. Improved thermal stability was successfully achieved by using PTMS and DEDMS as an encapsulating agent, and the PL quantum yield was almost independent of the annealing temperature below 160 ℃. The improved stability suggested that the sol-gel derived glass protected $Eu(FHA)_3(TPPO)_2$ from oxygen in the ambient air. In addition, the reduction of PL intensity during UV light irradiation was also suppressed by encapsulating in sol-gel glass, which was fabricated using PTMS and DEDMS. Measurements of the absorption coefficient indicate that the chemical bond between the Eu ion and the organic ligand was changed during high temperature annealing. The low PL quantum yield after high temperature annealing was responsible for the decrease in absorption by the organic ligand. Furthermore, the broad, intense excitation spectrum of the encapsulated samples suggests that no change occurs in the chemical structure of $Eu(HFA)_3(TPPO)_2$ during the sol-gel process. Such broad spectral output is an important factor for producing white LEDs with near-violet excitation.

References

[1] N. Kimura, K. Sakuma, S. Hirafune, K. Asano, N. Hirosaki, R.-J. Xie, Appl. Phys. Lett. 90 (2007) 051109.

[2] G. Gundiah, Y. Shimomura, N. Kijima, A.K. Cheetham, Chem. Phys. Lett. 455 (2008) 279-283.

[3] Z. Yan, L. Zhou, Y. Zhao, J. Wang, L. Huang, K. Hu, H. Liu, H. Wang, Z. Guo, Y. Song, H. Huang, R. Yang, Sens. Actuators B: Chem 119 (2006) 656-663.

[4] T. Trupke, A. Shalav, B.S. Richards, P. Würfel, M.A. Green, Solar Ener. Mater. Solar Cells 90 (2006) 3327-3338.

[5] T. Fukuda, S. Kato, E. Kin, K. Okaniwa, H. Morikawa, Z. Honda, N. Kamata, Opt. Mater. available online (doi:10.1016/j.optmat.2009.05.016)

[6] L.D. Carlos, R.A.S. Ferreira, V. Deermudez, S.J.L. Ribeiro, Adv. Mater. 21 (2009) 509-534.

[7] J. Kido, Y. Okamoto, Chem. Review 102 (2002) 1241-1245.

[8] T. Pagnot, P. Audebert, G. Tribillon, Chem. Phys. Lett. 322 (2000) 572-578.

[9] C.G. Gameiro, E.F. da Silva Jr., S. Alves Jr., G.F. de Sá, P.A. Santa-Cruz, J. Alloys Compd. 323-324 (2001) 820-823.

[10] P. Nockemann, E. Beurer, K. Driesen, R.V. Deun, K.V. Hecke, L.V. Meervelt, K. Binnemans, Chem. Comm. (2005) 4354-4356.

[11] P.P. Lima, R.A.S. Ferreira, R.O. Freire, F.A.A. Paz, L. Fu, S. Alves Jr., L.D. Carlos, O.L. Malta, Chem. Phys. Chem. 7 (2006) 735-746.

[12] H. Peng, C. Wu, Y. Jiang, S. Huang, J. McNeill, Langmuir, 23 (2007) 1591-1595.

[13] M.-S. Zhang, W. Yin, Q. Su, H.-J. Zhang, Mater. Lett. 57 (2002) 940-945.

[14] H. Li, S. Inoue, K. Machida, G. Adachi, Chem. Mater. 11 (1999) 3171-3176.

[15] W. Strek, J. Sokolnicki, J. Legendziewicz, K. Maruszewski, R. Reisfeld, T. Pavich, Opt. Mater. 13 (1999) 41-46.

[16] L.C. Cides da Silva, T.S. Martins, M.S. Filho, E.E.S. Teotônio, P.C. Isolani, H.F. Brito, M.H. Tabacniks, M.C.A. Fantini, J.R. Matos, Micro. Meso. Mater. 92 (2006) 94-100.

[17] E. Kin, T. Fukuda, S. Kato, Z. Honda, N. Kamata, J. Sol-Gel Sci. Technol. 50 (2009) 409-414.

[18] G. Qian, M. Wang, J. Am. Ceram. Soc. 83 (2000) 703-708.

[19] Y. Hasegawa, H. Kawai, K. Nakamura, N. Yasuda, Y. Wada, S. Yanagida, J. Alloys Compd. 408-412 (2006) 669-674.

[20] J.C. de Mello, H.F. Wittmann, R.H. Friend, Adv. Mater. 9 (1997) 230-232.

[21] K. Binnemans, P. Lenaerts, K. Driesen, C. Görller-Walrand, J. Mater. Chem. 14 (2004)?@191-195.

[22] T. Jin, S. Inoue, K. Machida, G. Adachi, J. Alloys and Compd. 265 (1998) 234-239.

[23] H. Eilers, B.M. Tissue, Chem. Phys. Lett. 251 (1996) 74-78.

[24] J. Fang, D. Ma, Appl. Phys. Lett. 83 (2003) 4041-4043.

Figure captions

Figure 1 Fabrication flowchart of the sol-gel glass encapsulated $Eu(HFA)_3(TPPO)_2$.

Figure 2 Optical microscopic images of samples A and B. PTMS:DEDMS and TMOS:DEDMS were used as the encapsulation agent.

Figure 3 (a) PL and (b) PLE spectra of the spin-coated and encapsulated samples.

Figure 4 Relationship between the PL quantum yield for 375 nm excitation and the annealing temperature.

Figure 5 Change in PL intensity with time under 350 nm excitation at 6.95 mW/cm^2 for $Eu(HFA)_3(TPPO)_2$ with and without encapsulation.

Figure 6 Influence of the annealing temperature on the change in PL intensity for sample A encapsulated by the sol-gel glass using PTMS and DEDMS under 350 nm excitation at 6.95 mW/cm^2.

Figure 7 (a) Absorption spectra of sample A for different annealing temperatures. (b) Relationship between the annealing temperature and the absorption coefficient of sample A at 350 nm.

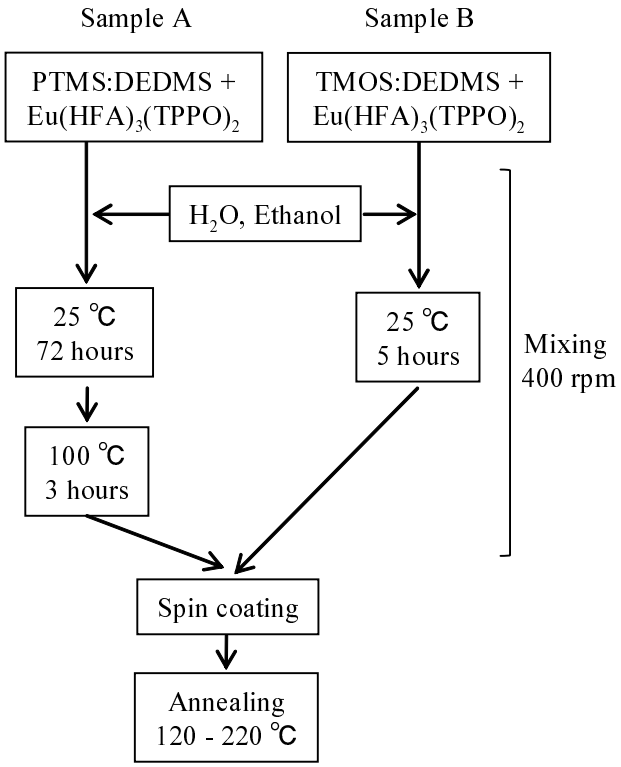

Figure 1: Fabrication flowchart of the sol-gel glass encapsulated $Eu(HFA)_3(TPPO)_2$.

Table 1: Molar ratios of starting solutions for sol-gel encapsulation.

Name	Silane agent	H_2O	Ethanol	$Eu(HFA)_3(TPPO)_2$
Sample A	PTMS:DEMDS=1:0.5	25	10	0.0015
Sample B	TMOS:DEDMS=1:0.5	5	10	0.0015

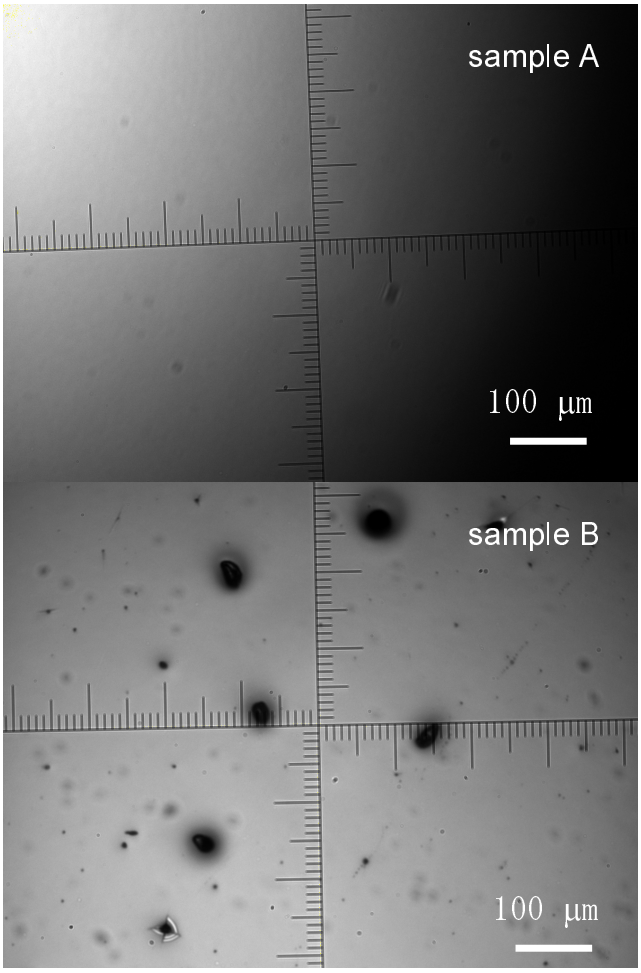

Figure 2: Optical microscopic images of samples A and B. PTMS:DEDMS and TMOS:DEDMS were used as the encapsulation agent.

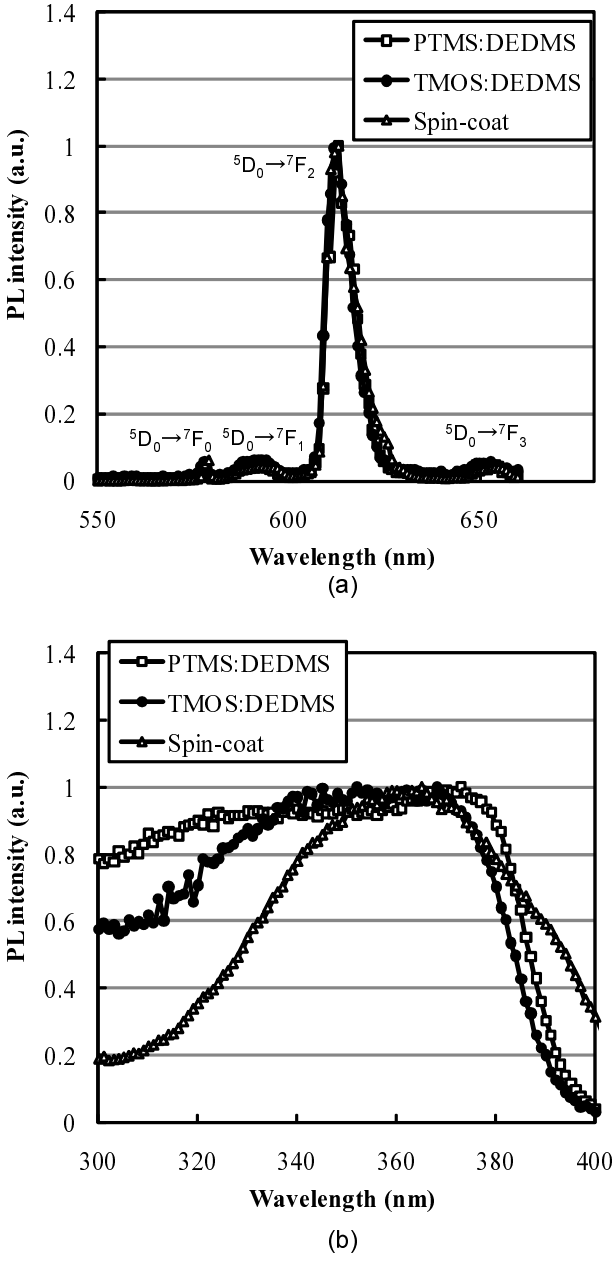

Figure 3: (a) PL and (b) PLE spectra of the spin-coated and encapsulated samples.

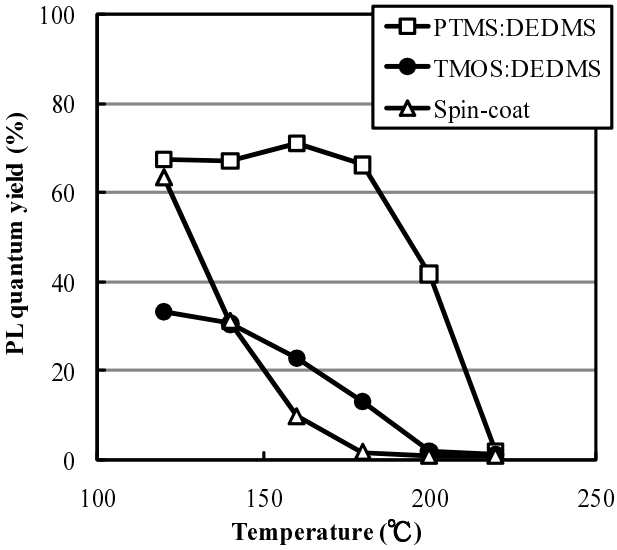

Figure 4: Relationship between the PL quantum yield for 375 nm excitation and the annealing temperature.

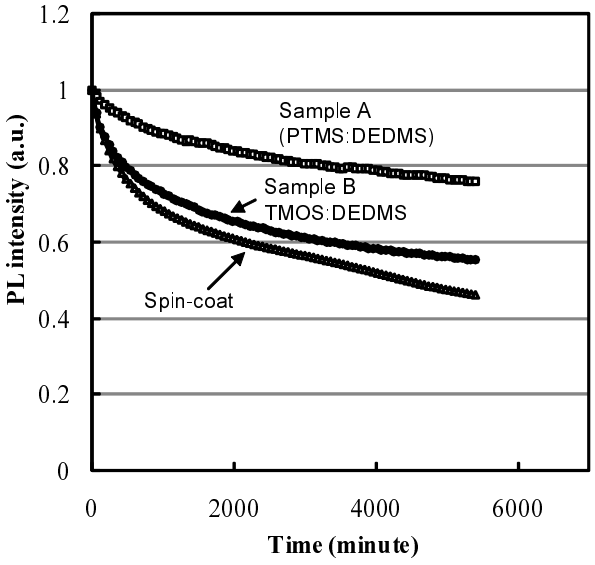

Figure 5: Change in PL intensity with time under 350 nm excitation at 6.95 mW/cm^2 for $Eu(HFA)_3(TPPO)_2$ with and without encapsulation.

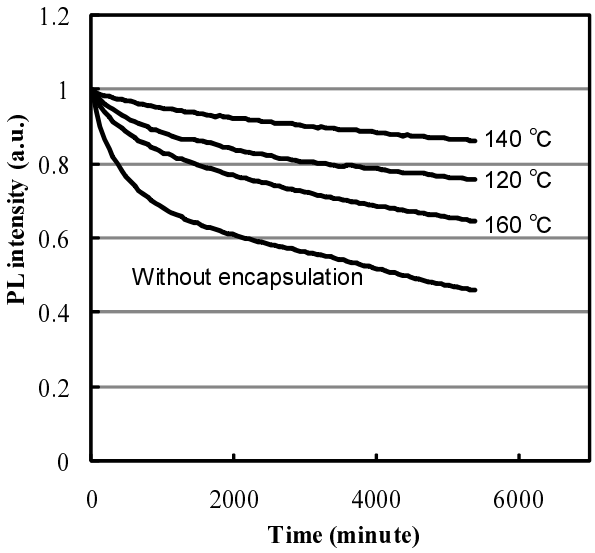

Figure 6: Influence of the annealing temperature on the change in PL intensity for sample A encapsulated by the sol-gel glass using PTMS and DEDMS under 350 nm excitation at 6.95 mW/cm^2.

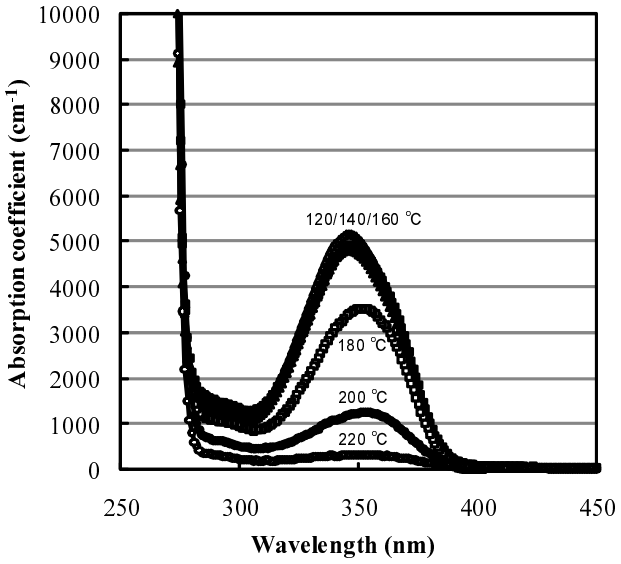

Figure 7: (a) Absorption spectra of sample A for different annealing temperatures. (b) Relationship between the annealing temperature and the absorption coefficient of sample A at 350 nm.